Low-temperature properties of an Yb impurity in a metallic host with an axial crystalline field

J. W. Rasul* and P. Schlottmann
Department of Physics, Temple University, Philadelphia, Pennsylvania 19122
(Received 2 September 1988)

The Bethe-*Ansatz* equations for the ground state of the Coqblin-Schrieffer model for $j=\frac{7}{2}$ are solved for a special axial-crystal-field-splitting scheme. The occupations of the crystal-field levels, the specific-heat contribution linear in the temperature, and the magnetic susceptibility parallel and perpendicular to the crystal axis are obtained as a function of the crystal-field strength. The universality of the results is discussed and a comparison with experiments on $YbCu_2Si_2$ and YbCuAl is made.

I. INTRODUCTION

Crystalline electric fields are known to quench the orbital angular momentum of magnetic ions, lifting in this way the degeneracy of the Hund's-rule ground multiplet. In the case of Yb^{3+} ions the total angular momentum of the ground state is $j=\frac{7}{2}$. A cubic crystalline field splits the octuplet into two doublets (Γ_6, Γ_7) and a quartet (Γ_8) and the small-magnetic-field susceptibility remains isotropic. Axial crystal fields, on the other hand, give rise to four Kramers doublets and the magnetic susceptibility is in general anisotropic, i.e., different for a small magnetic field parallel or perpendicular to the principal crystal axis. The system has a singlet ground state as a consequence of a Kondo spin-compensation, for all crystal-field-splitting schemes. Fermi-liquid arguments are then valid and the susceptibilities are always finite and at low T the specific heat is proportional to the temperature, with proportionality constant γ. All three quantities $\chi_{\parallel}$, $\chi_{\perp}$, and γ are functions of the splitting scheme and the strength of the crystal field. With increasing splitting there is a gradual crossover from the behavior of an isotropic octuplet for a small crystal field to that of a doublet for large axial crystal fields.

The thermal properties of these two extreme cases are very different. As a consequence of the spin compensation (Kondo effect) in the ground state, the low-energy excitation spectrum shows a peak known as the Kondo resonance. The position of the Kondo resonance determines the low-temperature thermodynamics: the peak is well above the Fermi level for an octuplet, but on resonance with the Fermi level for a doublet. The qualitative changes as a function of the crystal-field strength can in this way be understood in terms of a qualitative change in the Kondo resonance.

Exact results for a general crystal-field splitting scheme yielding four Kramers doublets are very tedious to obtain, but can be extracted analytically from the Bethe-*Ansatz* equations for special relations between the crystal-field energies. The purpose of this paper is to obtain the low-temperature properties of the impurity for the special choice of crystal-field parameters for which the energy differences between the Kramers doublets should be $1:\sqrt{2}:1$.

Our starting point are the Bethe-*Ansatz* equations for the Coqblin-Schrieffer model, which have been obtained independently by Tsvelick and Wiegmann,[1] Rasul,[2] and Andrei, Furuya, and Lowenstein.[3] These equations also correspond to the stable magnetic moment limit in the Bethe-*Ansatz* equations of the SU(N) Anderson model.[4] For $N=8$ they consist of seven linearly coupled integral equations of the Wiener-Hopf type, determining the seven relative occupations of the impurity levels as a function of the seven integration limits. For an arbitrary splitting scheme then these seven integration limits are all different and the coupled integral equations must be solved numerically. Within our special choice of splitting scheme only one integration limit is relevant and the system of equations can be solved by the standard Wiener-Hopf technique.

The effect of crystal fields on magnetic impurities in metals has been previously analyzed within the framework of Bethe's *Ansatz* for various cases. The occupation of the crystal-field levels, the magnetic susceptibility,[5] and the specific heat[6] were obtained for a $j=\frac{5}{2}$ impurity (Ce^{3+}) in cubic symmetry. The interplay of valence fluctuations and cubic-crystal-field splittings for $j=\frac{5}{2}$ has been discussed in Ref. 7. The specific heat of a quartet split into two Kramers doublets was calculated in Refs. 8 and 9. Finally, the effect of an axial crystal field splitting the Ce^{3+} sextuplet into three equally spaced Kramers doublets on the occupation of the levels, the susceptibility,[10] and the specific heat[9] has also been studied. This last example is closely related to the case presented here, which actually is its extension to Yb^{3+} impurities. Although the splitting scheme used is not a general one, our results are expected to give valuable information with possible application to systems such as $YbCu_2Si_2$.

The rest of the paper is organized as follows. In Sec. II we restate the ground state Bethe-*Ansatz* equations for the Coqblin-Schrieffer model and briefly discuss the relation between the integration limits and the splitting scheme. The situation of four Kramers doublets with a relative splitting of $1:\sqrt{2}:1$ is solved in Sec. III in the absence of a magnetic field and the population of the levels is obtained as a function of crystal-field strength. In Sec.

IV, the γ coefficient of the specific heat is calculated and including a small magnetic field in addition to the crystal field we obtain the magnetic susceptibility. The magnetic susceptibility is anisotropic and contains van Vleck terms. A discussion of the results follows in Sec. V, together with a comparison to Mössbauer measurements of the quadrupolar moment of the $4f$ shell of Yb in $YbCu_2Si_2$ and YbCuAl.

II. EQUATIONS AND GENERAL CONSIDERATIONS

Yb^{3+} impurities embedded in a simple metallic host are usually described in terms of the Coqblin-Schrieffer Hamiltonian

$$H=\sum_{km}\varepsilon_k C^\dagger_{km}C_{km}+J\sum_{\substack{k,k'\\m,m'}} C^\dagger_{km}f^\dagger_{m'}f_m C_{k'm'}\ , \tag{2.1}$$

where $C^\dagger_{km}$ creates a conduction electron of momentum $k=|\mathbf{k}|$ and total angular momentum component m $|m|\le j=\frac{7}{2}$, and similarly $f^\dagger_m$ creates a localized f electron. For convenience we have interchanged electrons with holes. The first term in (2.1), represents the kinetic energy and J is the exchange coupling constant.

The model (2.1) is soluble for a dispersion that is linearized around the Fermi level.[1-3] Since $j=\frac{7}{2}$ the impurity has $N=2j+1=8$ levels with the constraint that $\sum_m f^\dagger_m f_m=1$, i.e., with seven internal degrees of freedom. The exact solution is then obtained in terms of seven nested Bethe *Ansätze,* each of which eliminates one internal degree of freedom. Each Bethe-*Ansatz* generates a set of rapidities and these sets are interrelated by the Bethe-*Ansatz* equations. For the ground state these rapidities are all real and are conveniently described by density functions $\sigma^{(l)}(\xi)$, $l=1,\ldots,2j$ in the thermodynamic limit. The energy of the system expressed in the terms of the rapidities is

$$E=\sum_{l=1}^{2j} l\int d\xi\,\xi\sigma^l(\xi)\ , \tag{2.2}$$

so that it is energetically favorable to occupy all states with rapidities in the interval $(-\infty,B_l)$. It is usual to introduce "hole"-distribution functions $\sigma^{(l)}_h(\xi)$, which are complementary to the $\sigma^{(l)}(\xi)$, i.e., they vanish in the interval $(-\infty,B_l)$. Particle and hole densities are linearly related by the following Wiener-Hopf integral equations:

$$\sigma^l_h(\xi)+\sum_{q=1}^{2j}\int_{-\infty}^{B_q} d\xi'\,\sigma^{(q)}(\xi')K^j_{lq}(\xi-\xi')$$
$$=\frac{1}{2\pi}\int_{-\infty}^{\infty} dx e^{-iqx}\frac{\sinh[\frac{1}{2}x(2j+1-l)]}{\sinh[\frac{1}{2}x(2j+1)]}$$
$$\times\left[1+\frac{1}{L}\exp\left[-i\frac{x}{J}\right]\right]\ , \tag{2.3}$$

where $K_{lq}(\xi)$ is the Fourier transform of

$$K_{lq}(x)=e^{|x|/2}\sinh[\tfrac{1}{2}x(2j+1-\max\{l,q\})]$$
$$\times\frac{\sinh(\frac{1}{2}x\min\{l,q\})}{\sinh(\frac{1}{2}x)\sinh[\frac{1}{2}x(2j+1)]} \tag{2.4}$$

and L is the length of the box. The right-hand side consists of the driving terms of the equations; the term proportional to $1/L$ is the impurity term, while the extensive term corresponds to the free-electron gas. The density functions can then be separated into an impurity and a host part, $\sigma^{(l)}=\sigma^{(l)}_{\text{host}}+(1/L)\sigma^{(l)}_{\text{imp}}$. Note that the integral equations for impurity and host are formally very similar and the latter is obtained from the former in the limit $J\to\infty$.

Let us denote by n_l the occupation numbers of the impurity levels labeled in decreasing order, $n_1\ge n_2\ge\cdots\ge n_{2j}\ge n_{2j+1}\ge 0$, such that n_1 corresponds to the lowest-lying level and n_{2j+1} is the least populated. Similar relations can be defined for the populations N_l in the electron gas. The density function $\sigma^{(l)}(\xi)$ is associated with all $n_q(N_q)$ for $q\le l$ occupied and $q>l$ empty. The relative occupation of the impurity levels is then given by

$$n_l-n_{l+1}=\int_{-\infty}^{B_l} d\xi\,\sigma^{(l)}_{\text{imp}}(\xi)\ ,\quad n_{2j+2}=0 \tag{2.5}$$

and similar relations hold for the host.

The B_l are a set of $2j$ constants to be determined by the external conditions imposed on the impurity. They determine the number of electrons of each "color" in the host and hence the relative population of the impurity levels. The splitting of a $(2j+1)$-fold multiplet can be expressed as a linear combination of Stevens operators O_l, where $1\le l\le 2j$. In the ionic Hamiltonian of the impurity there are then $2j$ independent coefficients which uniquely determine the B_l. The Zeeman splitting, for instance, can be characterized by an O_1 Stevens operator and is the only possible splitting for a spin $\frac{1}{2}$. A triplet can in addition be split by an axial crystal field, i.e., and O_2 Stevens operator. The degeneracy of a quartet can be lifted with an arbitrary splitting between the levels by means of the axial crystal fields O^0_2 and O^2_2 and a magnetic field.

We diagonalize the ionic f Hamiltonian and new eigenstates (colors) replace the spin eigenstates. It is assumed that the host has a splitting similar to that of the impurity, such that the number of electrons of each color is a conserved quantity of the system (host with impurity). This assumption is not restrictive if the bandwidth is much larger than the splittings. The corrections induced are then of the order of the splitting divided by the bandwidth and hence negligible. Equations (2.3)–(2.5) remain unchanged when reinterpreted in terms of colors. Hence the splitting scheme of the isolated ion completely determines that of the interacting system, i.e., in the presence of the Kondo effect. This paper is devoted to the situation of Yb^{3+}, i.e., $j=\frac{7}{2}$, for which we briefly discuss three examples to illustrate the above general discussion.

(a) In a *pure Zeeman* splitting[11] all degeneracies are lifted such that, according to (2.5), all $B_l=-\infty$. The parameters B_l are determined such that for small fields, n_l-n_{l+1} in (2.5) is proportional to H and independent of l. From the symmetries of the kernel of the integral

equations we have then that $B_1=B_7$, $B_2=B_6$, and $B_3=B_5$. Only one B_l, e.g., B_1, is independent and parametrizes the field, $B_1=4\ln(H/\varepsilon_F)/\pi$, where ε_F is the Fermi energy. The remaining B_l have been found numerically[11] to be given by $B_2=B_1+0.255$, $B_3=B_1+0.388$, and $B_4=B_1+0.430$.

(b) In a *cubic environment* the octuplet splits into a Γ_6 doublet, a Γ_7 doublet, and a Γ_8 quartet. Only two of the B_l parameters are then different from $-\infty$ ($B_l=-\infty$ for odd l). Two parameters, a fourth-order and a sixth-order one, determine the splitting[12] such that the problem reduces to a numerical solution of two coupled linear integral equations of the Wiener-Hopf type. The ground multiplet is always a doublet, so that B_2 is always finite.

(c) In a pure *axial crystal field* the $j=\frac{7}{2}$ splits into four Kramers doublets and hence $B_l=-\infty$ for odd l. The parameters B_2, B_4, and B_6 are finite and are determined by the second-, fourth-, and sixth-order Stevens operators in the ionic scheme. In this case three Wiener-Hopf integral equations remain and must in general be solved numerically.

The integral equations for cases (b) and (c) can, however, be solved analytically in some special situations, namely, when the integration limits B_l different from $-\infty$ are equal. In case (c), i.e., for an axial crystal field, this corresponds to crystal-field excitation energies from the Kramers ground doublet of Δ, $(1+\sqrt{2})\Delta$, and $(2+\sqrt{2})\Delta$. The solution of this situation is presented in the next two sections. Although this represents a special splitting scheme we believe that the conclusions drawn are generally more valid.

III. $j=\frac{7}{2}$ IN AXIAL SYMMETRY AND ZERO MAGNETIC FIELD

We consider the integral equations (2.3) for the situation in which $B_1=B_3=B_5=B_7=-\infty$ and $B_2=B_4=B_6=B$. This corresponds to a splitting of the octuplet into four Kramers doublets with crystal-field excitation energies Δ, $(1+\sqrt{2})\Delta$, and $(2+\sqrt{2})\Delta$. The energy Δ determines the integration limit B; this relation is derived below. B grows monotonically with Δ, being $-\infty$ for $\Delta=0$. Equations (2.3) reduce to three coupled Wiener-Hopf integral equations for the density functions $\sigma^{(2)}$, $\sigma^{(4)}$, and $\sigma^{(6)}$. Since the integration limits are all equal, this system of equations exactly decouples into three single integral equations. In view of the symmetries of the kernel we introduce the following linear combinations of the density functions:

$$\rho_1(\xi)=\frac{1}{\sqrt{2}}[\sigma^{(2)}(\xi)+\sigma^{(6)}(\xi)+\sqrt{2}\sigma^{(4)}(\xi)]\ , \tag{3.1a}$$

$$\rho_2(\xi)=\frac{1}{\sqrt{2}}[\sigma^{(2)}(\xi)+\sigma^{(6)}(\xi)-\sqrt{2}\sigma^{(4)}(\xi)]\ , \tag{3.1b}$$

$$\rho_3(\xi)=\frac{1}{\sqrt{2}}[\sigma^{(2)}(\xi)-\sigma^{(6)}(\xi)]\ , \tag{3.1c}$$

and analogous expressions for the hole functions. The densities diagonalize the kernel K_{lq}, Eq. (2.4) for $l,q=2,4,6$, such that the integral equations take the form

$$\rho_{ih}(\xi)+\int_{-\infty}^{B}d\xi'\,\rho_i(\xi')K_i(\xi-\xi')=g_i(\xi)\ , \tag{3.2}$$

where $K_i(\xi)$ are the Fourier transforms of

$$\hat{K}_1(x)=e^{|x|/2}[\cosh(x/2)/\cosh(2x)] \times 4\cosh(x/2+i\pi/8)\cosh(x/2-i\pi/8)\ , \tag{3.3a}$$

$$\hat{K}_2(x)=e^{|x|/2}[\cosh(x/2)/\cosh(2x)] \times 4\sinh(x/2+i\pi/8)\sinh(x/2-i\pi/8)\ , \tag{3.3b}$$

$$\hat{K}_3(x)=e^{|x|/2}\cosh(x/2)/\cosh x\ , \tag{3.3c}$$

and $g_i(\xi)$ are the corresponding driving terms, which are given by the Fourier transform of

$$\hat{g}_1(x)=\sqrt{2}\left[1+\frac{1}{L}\exp\left[\frac{-ix}{J}\right]\right]\cosh(x/2+i\pi/8) \times\cosh(x/2-i\pi/8)/\cosh(2x)\ , \tag{3.4a}$$

$$\hat{g}_2(x)=\sqrt{2}\left[1+\frac{1}{L}\exp\left[\frac{-ix}{J}\right]\right]\sinh(x/2+i\pi/8) \times\sinh(x/2-i\pi/8)/\cosh(2x)\ , \tag{3.4b}$$

$$\hat{g}_3(x)=2^{-3/2}\left[1+\frac{1}{L}\exp\left[\frac{-ix}{J}\right]\right]\Big/\cosh x\ . \tag{3.4c}$$

We solve the Wiener-Hopf integral equations following the standard procedure.[13] The kernels $K_i(x)$ are written as a product of two functions $K_i(x)=G_i^+(x)G_i^-(x)$, where $G_i^-(x)=G_i^+(-x)$, $G_i^+(x)$ approaches a constant as $x\to\infty$, and $G_i^+(x)$ [$G_i^-(x)$] is analytic in the upper (lower) complex half-plane. The function $G_i^+(x)$, obtained from Eqs. (3.3), is given by

$$G_1^+(x)=2\pi[(-ix+0)/a_1]^{ix/2\pi} \times\frac{\Gamma(\frac{1}{2}-i2x/\pi)}{\Gamma(\frac{1}{2}-ix/2\pi)\Gamma(\frac{5}{8}-ix/2\pi)\Gamma(\frac{3}{8}-ix/2\pi)}\ , \tag{3.5a}$$

$$\hat{g}_2(x)=2\pi[(-ix+0)/a_2]^{ix/2\pi} \times\frac{\Gamma(\frac{1}{2}-i2x/\pi)}{\Gamma(\frac{1}{2}-ix/2\pi)\Gamma(\frac{1}{8}-ix/2\pi)\Gamma(\frac{7}{8}-ix/2\pi)}\ , \tag{3.5b}$$

$$\hat{g}_3(x)=[(-ix+0)/a_3]^{ix/2\pi}\frac{\Gamma(\frac{1}{2}-ix/\pi)}{\Gamma(\frac{1}{2}-ix/2\pi)}\ , \tag{3.5c}$$

where $a_1=a_2=e\pi/2^7$ and $a_3=\pi e/2$. Here 0 denotes an infinitesimal. The Wiener-Hopf equations can now be rewritten as

$$\hat{\rho}_{ih}(x)/G_i^+(x)+\hat{\rho}_i(x)G_i^-(x)=\hat{g}_i(x)/G_i^+(x)\ . \tag{3.6}$$

The first term on the left-hand side is analytic in the upper complex half-plane, while the second one is analytic in the lower half-plane. A similar separation can be

done on the right-hand side of (3.6) by means of a Cauchy transform. These two solutions (analytic in the upper and lower half-planes, respectively) coincide on an infinitesimal strip around the real axis, so that one can be considered the analytic continuation of the other. In this way we obtain

$$\hat{\rho}_{ih}(x)=G_i^+(x)\int \frac{dy}{2i\pi}\frac{\hat{g}_i(y)e^{-iBy}}{y-x-i0}\frac{1}{G_i^+(y)}\ , \tag{3.7a}$$

$$\hat{\rho}_i(x)=-\frac{1}{G_i^-(x)}\int \frac{dy}{2i\pi}\frac{\hat{g}_i(y)e^{-iBy}}{y-x+i0}\frac{1}{G_i^+(y)}\ . \tag{3.7b}$$

Note that each ρ_i and ρ_{ih} consists of a host and an impurity part. The number of electrons with a given crystal-field symmetry is obtained from (3.7b) for $x=0$ via Eqs. (2.5) and (3.1). The impurity part of (3.7b) for $x=0$ can be rewritten in a more convenient way by making use of (3.4) and (3.5):

$$\hat{\rho}_{1\,\mathrm{imp}}(0)=-\frac{1}{2i\pi}[2^{3/2}\sin(3\pi/8)]^{-1}\int_{-\infty}^{\infty}dy\frac{\exp[-iy(B+1/J)]}{y+i0}\left[\frac{-iy+0}{(e\pi/2^7)}\right]^{-iy/2\pi}\frac{\Gamma(\frac{1}{2}+i2y/\pi)\Gamma(\frac{1}{2}-iy/2\pi)}{\Gamma(\frac{3}{8}+iy/2\pi)\Gamma(\frac{5}{8}+iy/2\pi)}\ , \tag{3.8a}$$

$$\hat{\rho}_{2\,\mathrm{imp}}(0)=-\frac{1}{2i\pi}[2^{7/2}\sin(\pi/8)]^{-1}\int_{-\infty}^{\infty}dy\frac{\exp[-iy(B+1/J)]}{y+i0}\left[\frac{-iy+0}{(\pi e/2^7)}\right]^{-iy/2\pi}\frac{\Gamma(\frac{3}{2}+i2y/\pi)\Gamma(\frac{1}{2}-iy/2\pi)}{\Gamma(\frac{7}{8}+iy/2\pi)\Gamma(\frac{9}{8}+iy/2\pi)}\ , \tag{3.8b}$$

$$\hat{\rho}_{3\,\mathrm{imp}}(0)=-\frac{1}{2i\pi}(2^{3/2}\pi)^{-1}\int_{-\infty}^{\infty}dy\frac{\exp[-iy(B+1/J)]}{y+i0}\left[\frac{-iy+0}{\pi e/2}\right]^{-iy/2\pi}\Gamma(\tfrac{1}{2}-iy/2\pi)\Gamma(\tfrac{1}{2}+iy/\pi)\ . \tag{3.8c}$$

Note that these expressions, as well as (3.7) for arbitrary x, are *universal* expressions as a function of $B+1/J$. The same expressions hold for the electron gas if J is set equal to ∞. For small crystal fields, $\Delta \ll T_K$ or $B+1/J \ll 0$, expressions (3.8) can be expanded in powers of $\exp(\pi B/4)$ by closing the contour through the upper half-plane. The contributions arise from the poles of $\Gamma(\frac{1}{2}+i2y/\pi)$, $\Gamma(\frac{3}{2}+i2y/\pi)$, and $\Gamma(\frac{1}{2}+iy/\pi)$, respectively. The pole closest to the real axis in each case determines the leading behavior for small Δ; these poles are at $i\pi/4$, $i3\pi/4$, and $i\pi/2$, respectively, giving rise to a linear dependence in Δ only for $\hat{\rho}_1(0)$ [note that $\hat{\rho}_2(0)\sim\Delta^3$ and $\hat{\rho}_3(0)\sim\Delta^2$]. Since Δ is always much smaller than ε_F, the linear approximation to $\hat{\rho}_{1\,\mathrm{host}}(0)$ can be used to relate Δ and B. From the definition of ρ_1 [Eq. (3.1a)] and (2.5) we have that

$$\begin{aligned}\hat{\rho}_{1\,\mathrm{host}}(0)&=\frac{1}{\sqrt{2}}[\hat{\sigma}^{(2)}_{\mathrm{host}}(0)+\hat{\sigma}^{(6)}_{\mathrm{host}}(0)+\sqrt{2}\hat{\sigma}^{(4)}_{\mathrm{host}}(0)]\\&=\frac{1}{\sqrt{2}}[N_2-N_8+(\sqrt{2}-1)(N_4-N_6)]\\&=\left[\frac{2}{e}\right]^{1/8}[\pi^{1/2}\sin(3\pi/8)]^{-1}\\&\quad\times[\Gamma(\tfrac{5}{8})/\Gamma(\tfrac{1}{4})]\exp(\pi B/4)\end{aligned} \tag{3.9}$$

(recall that $N_1=N_2$, $N_3=N_4$, $N_5=N_6$, and $N_7=N_8$), which in linear response is to be equated to $2\sqrt{2}(\Delta/2\varepsilon_F)$, where $1/2\varepsilon_F$ is the density of states of the host. Hence B is roughly given by $(N/2\pi)\ln(\Delta/\varepsilon_F)$, with $N=2j+1=8$. It is also easily verified that for small Δ

$$n_2-n_4=\frac{1}{\sqrt{2}}(n_4-n_6)=(n_6-n_8)\sim\Delta\ ,$$

as expected from our splitting scheme.

For large Δ, i.e., $\Delta \gg T_K$, the contour has to be closed through the lower half-plane. As expected, $n_1=n_2$ asymptotically approaches the value $\frac{1}{2}$, while the occupations of the other levels tend to zero. The deviations from these saturation values are logarithmic, characteristic of asymptotic freedom in the Kondo problem.

The populations of the impurity levels as a function of $\Delta/T_K^{(8)}$ are shown in Fig. 1. Here $T_K^{(8)}$ refers to the Kondo temperature of the degenerate octuplet, $T_K^{(8)}=\varepsilon_F\exp(-\pi/4J)$, defined such that the magnetic susceptibility of the octuplet at $T=0$ is $\chi=j(j+1)/3T_K=21/4T_K$. The response of the multiplet to changes of the crystal-field strength Δ, i.e., the derivative of the energy with respect to Δ, is given by

$$q(\Delta)=\hat{\rho}_{1\,\mathrm{imp}}(0)=\frac{1}{\sqrt{2}}[n_2-n_8+(\sqrt{2}-1)(n_4-n_6)]\ . \tag{3.10}$$

This expression is linear in Δ for small crystalline fields and approaches asymptotically on a logarithmic scale its saturation value $q_{\mathrm{sat}}=1/2\sqrt{2}$ for large Δ. A plot of q/q_{sat} is shown in Fig. 2. It is interesting to note that the linear regime of $q(\Delta)$ extends beyond $\Delta/T_K^{(8)}=0.12$ and deviations from the straight line at $\Delta/T_K^{(8)}=0.15$ are only of the order of 3%. A similar large linear regime was found previously with respect to a Zeeman splitting of the octuplet.

IV. SPECIFIC HEAT AND ANISOTROPIC MAGNETIC SUSCEPTIBILITY

In order to obtain the magnetic susceptibility we add a small magnetic field to our splitting scheme. The mag-

netic field lifts all remaining degeneracies, i.e., splits the Kramers doublets. Hence all integration limits B_l, $l=1,2,..,7$, are now finite, but since the Zeeman energy for a small field is much smaller than the crystal splittings and the Kondo temperature, we have that

$$B_1,B_3,B_5,B_7 \ll B_2,B_4,B_6 \ .$$

The susceptibility is obtained in linear response to the magnetic field. It is then convenient to express the integral equations in terms of the density functions $\sigma^{(1)}$, $\sigma^{(3)}$, $\sigma^{(5)}$, and $\sigma^{(7)}$ and the hole-density functions $\sigma_h^{(2)}$, $\sigma_h^{(4)}$ and $\sigma_h^{(6)}$. For this purpose we eliminate $\sigma^{(2)}$, $\sigma^{(4)}$, and $\sigma^{(6)}$ from the integral equations (2.3) for $l=1$, 3, 5, and 7.

Consider the integral equations (2.3) for $l=2$, 4, and 6. In order to invert this system of equations we form the linear combinations (3.1) which diagonalize the kernel of this subspace and Fourier transform. The inversion is now straightforward and after some tedious algebra we obtain

$$\hat{\sigma}^{(2)}(\omega)=\left[-\hat{\sigma}_h^{(2)}(\omega)e^{-|\omega|/2}2\cosh\omega+\hat{\sigma}_h^{(4)}(\omega)e^{-|\omega|/2}+\left[1+\frac{1}{L}e^{-i\omega/J}\right]e^{-|\omega|/2}-\hat{\sigma}^{(1)}(\omega)-\hat{\sigma}^{(3)}(\omega)\right]\Big/2\cosh(\omega/2)\ , \tag{4.1a}$$

$$\hat{\sigma}^{(4)}(\omega)=\{[\hat{\sigma}_h^{(2)}(\omega)+\hat{\sigma}_h^{(6)}(\omega)]e^{-|\omega|/2}-\hat{\sigma}_h^{(4)}(\omega)e^{-|\omega|/2}2\cosh\omega-\hat{\sigma}^{(3)}(\omega)-\hat{\sigma}^{(5)}(\omega)\}/2\cosh(\omega/2)\ , \tag{4.1b}$$

$$\hat{\sigma}^{(6)}(\omega)=[\hat{\sigma}_h^{(4)}(\omega)e^{-|\omega|/2}-\hat{\sigma}_h^{(6)}(\omega)]e^{-|\omega|/2}2\cosh\omega-\hat{\sigma}^{(5)}(\omega)-\hat{\sigma}^{(7)}(\omega)]/2\cosh(\omega/2)\ . \tag{4.1c}$$

The above expressions are inserted into the other four integral equations (for odd values of l) yielding after Fourier transforming back into rapidities space

$$\sigma_h^{(l)}(\xi)+\int_{-\infty}^{\infty}d\xi'\sigma^{(l)}(\xi')\int_{-\infty}^{\infty}\frac{d\omega}{2\pi}\frac{\exp[i\omega(\xi-\xi')+\frac{1}{2}|\omega|]}{2\cosh(\omega/2)}=f_l(\xi)\ , \tag{4.2}$$

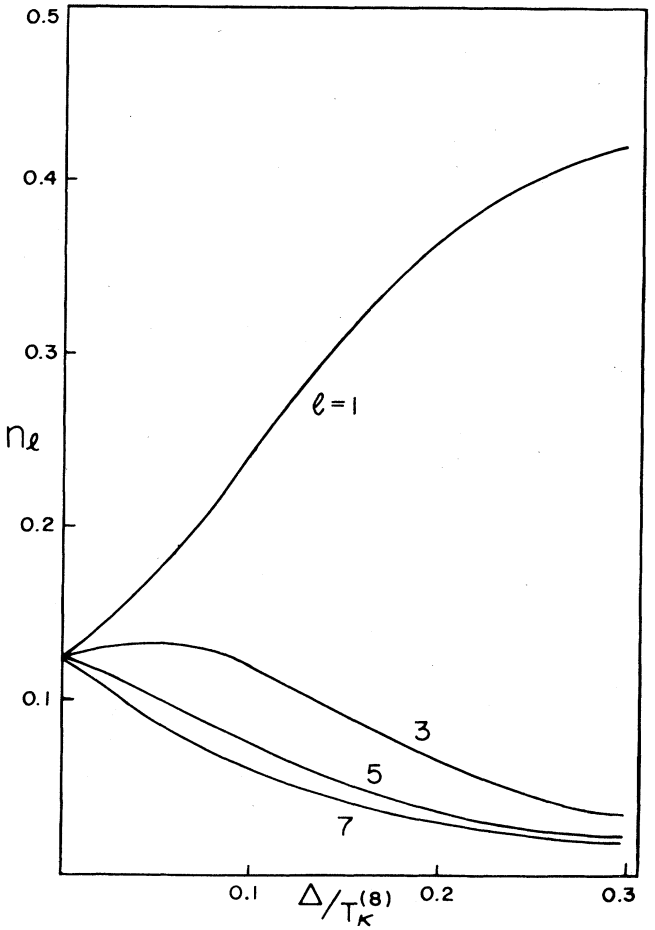

FIG. 1. Population of one level of each of the Kramers doublets as a function of the crystal-field strength over the Kondo temperature of the octuplet.

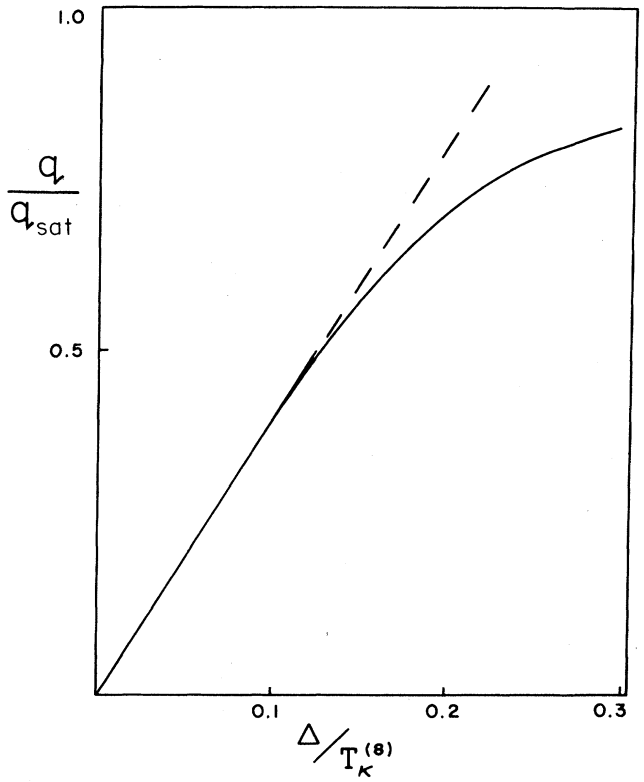

FIG. 2. Crystal-field response function $q(\Delta)$, defined by Eq. (3.10), over its saturation value $q_{sat}=1/2\sqrt{2}$ as a function of $\Delta/T_K^{(8)}$. The dashed line is the extrapolation of the linear regime.

where the driving terms $f_l(\xi)$ are the Fourier transforms of

$$\hat{f}_1(\omega)=\left[\left[1+\frac{1}{L}e^{-i\omega/J}\right]+\hat{\sigma}_h^{(2)}(\omega)\right]\Big/2\cosh(\omega/2)\ , \tag{4.3a}$$

$$\hat{f}_3(\omega)=[\hat{\sigma}_h^{(2)}(\omega)+\hat{\sigma}_h^{(4)}(\omega)]/2\cosh(\omega/2)\ , \tag{4.3b}$$

$$\hat{f}_5(\omega)=[\hat{\sigma}_h^{(4)}(\omega+\hat{\sigma}_h^{(6)}(\omega)]/2\cosh(\omega/2)\ , \tag{4.3c}$$

$$\hat{f}_7(\omega)=\hat{\sigma}_h^{(6)}(\omega)/2\cosh(\omega/2)\ . \tag{4.3d}$$

The hole functions corresponding to the densities associated with the crystal-field splittings, $\sigma_h^{(2)}$, $\sigma_h^{(4)}$, and $\sigma_h^{(6)}$, have been incorporated into the driving terms. Only the integral equation with $l=1$ has a Kondo driving term. The density $\sigma^{(1)}(\xi)$ describes the splitting of the lowest-lying Kramers doublet.

It is worth pointing out that for small magnetic fields the integral equations corresponding to the lifting of the degeneracy of the Kramers doublets are all independent and of the Wiener-Hopf type. In other words, the kernel does not couple different densities of odd index l. Moreover, the kernel is the same one as for a spin-$\frac{1}{2}$ Kondo impurity. The $[2\cosh(\omega/2)]^{-1}$ in the driving terms is also characteristic of the spin-$\frac{1}{2}$ Kondo problem.

Since we are interested in the linear response to a magnetic field, $B_l \ll 0$ (for l being odd) and only the asymptotic behavior as $\xi\to-\infty$ matters in the driving terms. The contour in the Fourier transform of the $\hat{f}_l(\omega)$ is then closed through the upper ω half-plane and the leading contribution arises from the pole of $[2\cosh(\omega/2)]^{-1}$ closest to the real axis, i.e., at $\omega=i\pi$. All $f_l(\xi)$ for $\xi\to-\infty$ are then proportional to $\exp(\pi\xi)$. The proportionality factors are, respectively,

$$\alpha_1=1+\frac{1}{L}e^{\pi/J}+\hat{\sigma}_h^{(2)}(i\pi)e^{-\pi B}\ , \tag{4.4a}$$

$$\alpha_3=[\hat{\sigma}_h^{(2)}(i\pi)+\hat{\sigma}_h^{(4)}(i\pi)]e^{-\pi B}\ , \tag{4.4b}$$

$$\alpha_5=[\hat{\sigma}_h^{(4)}(i\pi)+\hat{\sigma}_h^{(6)}(i\pi)]e^{-\pi B} \tag{4.4c}$$

$$\alpha_7=\hat{\sigma}_h^{(6)}(i\pi)e^{-\pi\beta}\ . \tag{4.4d}$$

The constants α_l consist of a host and an impurity contribution, since each of $\hat{\sigma}_h^{(l)}(i\pi)$, $l=2,4,6$, is a sum of such terms. Hence, the impurity and host solutions for $\sigma^{(l)}(\xi)$, $l=1,3,5,7$, are proportional, their ratio being given by

$$\sigma^{(l)}_{\rm imp}(\xi)/\sigma^{(l)}_{\rm host}(\xi)=\alpha_l({\rm imp})/\alpha_l({\rm host})\ . \tag{4.4e}$$

This relation is a consequence of the Fermi-liquid properties of the system. The expressions for $\hat{\sigma}^{(l)}_{h\,\rm imp}(i\pi)$, $l=2,4,6$, can be obtained from those for $\hat{\rho}_{ih\,\rm imp}(i\pi)$, $i=1,2,3$. For $x=i\pi$, Eq. (3.7b) yields

$$\hat{\rho}_{1h\,\rm imp}(i\pi)=\frac{1}{2i\pi}[\tfrac{3}{4}(e\pi)^{1/2}\sin\pi/8)]\int_{-\infty}^{\infty}dy\frac{\exp[-iy(B+1/J)]}{(y-i\pi)}\left[\frac{-iy+0}{(\pi e/2^7)}\right]^{-iy/2\pi}\frac{\Gamma(\frac{1}{2}+i2y/\pi)\Gamma(\frac{1}{2}-iy/2\pi)}{\Gamma(\frac{3}{8}+iy/2\pi)\Gamma(\frac{5}{8}+iy/2\pi)}\ , \tag{4.5a}$$

$$\hat{\rho}_{2h\,\rm imp}(i\pi)=\frac{1}{2i\pi}[\tfrac{1}{16}(e\pi)^{1/2}\sin(3\pi/8)]\int_{-\infty}^{\infty}dy\frac{\exp[-iy(B+1/J)]}{(y-i\pi)}\left[\frac{-iy+0}{(\pi e/2^7)}\right]^{-iy/2\pi}\frac{\Gamma(\frac{3}{2}+i2y/\pi)\Gamma(\frac{1}{2}-iy/2\pi)}{\Gamma(\frac{7}{8}+iy/2\pi)\Gamma(\frac{9}{8}+iy/2\pi)}\ , \tag{4.5b}$$

$$\hat{\rho}_{3h\,\rm imp}(i\pi)=\frac{1}{2i\pi}[\tfrac{1}{8}(e/\pi)^{1/2}]\int dy\frac{\exp[-iy(B+1/J)]}{(y-i\pi)}\left[\frac{-iy+0}{(\pi e/2)}\right]^{-iy/2\pi}\Gamma(\tfrac{1}{2}-iy/2\pi)\Gamma(\tfrac{1}{2}+iy/\pi)\ , \tag{4.5c}$$

and the corresponding expressions for the electron gas are obtained by taking $J\to\infty$.

In analogy to Eqs. (3.8) the small-crystal-field expansion is obtained by closing the integration contour through the upper half-plane from the pole at $y=i\pi$ and the poles of the Γ functions. Again only $\hat{\rho}_{1h}(i\pi)$ has a contribution linear in Δ,

$$\hat{\rho}_{1h\,\rm host}(i\pi)=(e/2)^{3/8}\sin(\pi/8)[\Gamma(\tfrac{5}{8})/\Gamma(\tfrac{1}{4})]\times\exp(\pi B/4)\ , \tag{4.6}$$

so that

$$\hat{\sigma}^{(2)}_{h\,\rm host}(i\pi)=\frac{1}{\sqrt{2}}\hat{\sigma}^{(4)}_{h\,\rm host}(i\pi)=\sigma^{(6)}_{h\,\rm host}(i\pi)=\frac{1}{2\sqrt{2}}\hat{\rho}_{1h\,\rm host}(i\pi)\ . \tag{4.7}$$

The large-crystal-field limit of $\hat{\rho}_{ih\,\rm imp}(i\pi)$ shows the expected logarithmic behavior as a function of $\Delta/T_k^{(8)}$.

The specific heat at low temperatures is proportional to T, as a consequence of the singlet ground state and the concomitant Fermi-liquid properties. The proportionality factor γ is thus determined by the ground-state density functions[14]

$$\gamma=\frac{\pi^2}{3}\frac{1}{N\varepsilon_F}\sum_{l=1}^{2j}[\sigma^{(l)}_{\rm imp}(B_l)/\sigma^{(l)}_{\rm host}(B_l)]\ . \tag{4.8}$$

Note that for $\Delta\to0$ the ratio of impurity and host densities becomes independent of l and equal to $\exp(\pi/4J)$, so

that the well-known result for the Coqblin-Schrieffer model is recovered:

$$N\gamma^{(8)}=2j\pi^2/3T_k^{(8)}\ ,\quad N=2j+1=8\ . \tag{4.9}$$

If $\Delta\neq 0$ we distinguish two types of contributions: (a) those arising from densities with odd l and (b) those from densities with even l. The contribution (a) to (4.8) can be written as

$$\frac{\pi^2}{24\varepsilon_F}\left[2^{3/2}\exp[\pi(B+1/J)]+\tfrac{8}{3}\hat{\rho}_{1h\,\mathrm{imp}}(i\pi)+\frac{4\sqrt{2}}{3}\hat{\rho}_{2h\,\mathrm{imp}}(i\pi)\right]\Big/\hat{\rho}_{1h\,\mathrm{host}}(i\pi)\ , \tag{4.10}$$

where all expressions have already been defined above. The remaining three terms are reformulated by means of the following property of the Fourier transform:

$$\sigma^{(l)}(B_l)=\lim_{\xi\to B_l-0}\sigma^{(l)}(\xi)=\lim_{x\to\infty}ix\hat{\sigma}^{(l)}(x)\ , \tag{4.11}$$

which are easily obtained from the expressions for $\rho_i(B)$, $i=1,2,3$,

$$\rho_{1\,\mathrm{imp}}(B)=\lim_{x\to\infty}ix\hat{\rho}_{1\,\mathrm{imp}}(x)=(\pi 2^{3/2})^{-1}\int_{-\infty}^{\infty}dy\,e^{-i(B+1/J)y}\left[\frac{-iy+0}{(\pi e/2^7)}\right]^{-iy/2\pi}\frac{\Gamma(\frac{1}{2}+i2y/\pi)\Gamma(\frac{1}{2}-iy/2\pi)}{\Gamma(\frac{3}{8}+iy/2\pi)\Gamma(\frac{5}{8}+iy/2\pi)}\ , \tag{4.12a}$$

$$\rho_{2\,\mathrm{imp}}(B)=\lim_{x\to\infty}ix\hat{\rho}_{2\,\mathrm{imp}}(x)=(\pi 2^{7/2})^{-1}\int_{-\infty}^{\infty}dy\,e^{-i(B+1/J)y}\left[\frac{-iy+0}{(\pi e/2^7)}\right]^{-iy/2\pi}\frac{\Gamma(\frac{3}{2}+i2y/\pi)\Gamma(\frac{1}{2}-iy/2\pi)}{\Gamma(\frac{7}{8}+iy/2\pi)\Gamma(\frac{9}{8}+iy/2\pi)}\ , \tag{4.12b}$$

$$\rho_{3\,\mathrm{imp}}(B)=\lim_{x\to\infty}ix\hat{\rho}_{3\,\mathrm{imp}}(x)=(\pi^2 2^{5/2})^{-1}\int_{-\infty}^{\infty}dy\,e^{-i(B+1/J)y}\left[\frac{-iy+0}{(e\pi/2)}\right]^{-iy/2\pi}\Gamma(\tfrac{1}{2}-iy/2\pi)\Gamma(\tfrac{1}{2}+iy/\pi)\ . \tag{4.12c}$$

The corresponding expressions for the host are obtained by setting $J=\infty$. For small crystal field Δ, again only $\rho_i(B)$ has a linear contribution, in Δ, given by

$$\rho_{1\,\mathrm{host}}(B)=\frac{\pi^{1/2}}{2}\left[\frac{2}{e}\right]^{1/8}[\Gamma(\tfrac{5}{8})/\Gamma(\tfrac{1}{4})]e^{\pi B/4} \tag{4.13}$$

and a relation analogous to (4.7) also holds. The contribution (b) can now be expressed as follows

$$\frac{\pi^2}{24\varepsilon_F}\sqrt{2}[(\sqrt{2}+1)\rho_{1\,\mathrm{imp}}(B)+(\sqrt{2}-1)\rho_{2\,\mathrm{imp}}(B)]/\rho_{1\,\mathrm{host}}(B)\ , \tag{4.14}$$

so that γ is finally given by the sum of Eqs. (4.10) and (4.14).

A plot of γ normalized to its value for no crystal-field splitting [$\gamma^{(8)}$, Eq. (4.9)] as a function of Δ is shown in Fig. 3(a). γ grows monotonically with the splitting, quadratically for small Δ, and asymptotically for large Δ only the first term of (4.10) remains. Here the three excited Kramers doublets are nearly frozen out and only contribute to a renormalization of the Kondo temperature associated with the lowest-lying doublet. The γ coefficient is then inversely proportional to the renormalized Kondo temperature of the ground doublet

$$T_k^{(2)}=\varepsilon_F(\varepsilon_F/\Delta)^3e^{-\pi/J}\ . \tag{4.15}$$

Similar renormalization factors have been found previously for other crystal field schemes.[5–10,15]

The magnetic susceptibility strongly depends on the choice of the crystal-field levels and requires further assumptions. We are going to discuss two different arrangements of Kramers doublets: in (a) we assume that the levels $l=1,2$ refer to the quantum numbers $m=\pm\frac{1}{2}$, $l=3,4$ to $m=\pm\frac{3}{2}$, $l=5,6$ to $m=\pm\frac{5}{2}$, and $l=7,8$ to $m=\pm\frac{7}{2}$, while in (b) we associate them in decreasing populations with $m=\pm\frac{7}{2}$, $\pm\frac{5}{2}$, $\pm\frac{3}{2}$, and $\pm\frac{1}{2}$, respectively. In addition, for both cases the situations of the magnetic field being parallel and perpendicular to the crystal-field axis have to be distinguished, since the susceptibility is anisotropic as a consequence of the crystal-field splitting.

If the magnetic field is parallel to the crystal-field axis the magnetization is straightforwardly obtained, since no van Vleck corrections arise e.g., for case (a),

$$S_z=\tfrac{1}{2}\int_{-\infty}^{\infty}d\xi\,\sigma^{(1)}(\xi)+\tfrac{3}{2}\int_{-\infty}^{\infty}d\xi\,\sigma^{(3)}(\xi)+\tfrac{5}{2}\int_{-\infty}^{\infty}d\xi\,\sigma^{(5)}(\xi)+\tfrac{7}{2}\int_{-\infty}^{\infty}d\xi\,\sigma^{(7)}(\xi)\ , \tag{4.16}$$

and similarly for case (b). For small magnetic field the magnetization is obtained by comparing impurity and electron-gas contributions using Eqs. (4.4), i.e, the Fermi-liquid properties of the system, without actually solving the integral equations for odd l. This yields

$$\chi_{\parallel}=\left[\tfrac{1}{4}[e^{\pi(B+1/J)}+\hat{\sigma}_{h\,\mathrm{imp}}^{(2)}(i\pi)]+\tfrac{9}{4}[\hat{\sigma}_{h\,\mathrm{imp}}^{(2)}(i\pi)+\hat{\sigma}_{h\,\mathrm{imp}}^{(4)}(i\pi)]\frac{\sqrt{2}-1}{3}+\tfrac{25}{4}[\hat{\sigma}_{h\,\mathrm{imp}}^{(4)}(i\pi)+\hat{\sigma}_{h}^{(6)}(i\pi)]\frac{\sqrt{2}-1}{3}+\tfrac{49}{4}\hat{\sigma}_{h\,\mathrm{imp}}^{(6)}(i\pi)\right]\Big/[2^{1/2}\varepsilon_F\hat{\rho}_{1h\,\mathrm{host}}(i\pi)] \tag{4.17a}$$

for case (a) and for case (b)

$$\chi_{\parallel}=\left\{\tfrac{49}{4}[e^{\pi(B+1/J)}+\hat{\sigma}^{(2)}_{h\,\mathrm{imp}}(i\pi)]+\tfrac{25}{4}[\hat{\sigma}^{(2)}_{h\,\mathrm{imp}}(i\pi)+\hat{\sigma}^{(4)}_{h\,\mathrm{imp}}(i\pi)]\frac{\sqrt{2}-1}{3}\right.$$
$$\left.+\tfrac{9}{4}[\hat{\sigma}^{(4)}_{h\,\mathrm{imp}}(i\pi)+\hat{\sigma}^{(6)}_{h\,\mathrm{imp}}(i\pi)]\frac{\sqrt{2}-1}{3}+\tfrac{1}{4}\hat{\sigma}^{(6)}_{h\,\mathrm{imp}}(i\pi)\right\}\Big/[2^{1/2}\varepsilon_F\hat{\rho}_{1h\,\mathrm{host}}(i\pi)]\ . \tag{4.17b}$$

In the small-Δ limit both expressions reduce to the well-known result $\chi^{(8)}=j(j+1)/3T_K^{(8)}=21/4T_K^{(8)}$. For large Δ, on the other hand, the relevant term is the Kondo exponential of the lowest-lying Kramers doublet, $\exp[\pi(B+1/J)]$. The parallel susceptibility is then roughly inversely proportional to the Kondo temperature of the fundamental doublet, Eq. (4.15). A plot of $\chi_{\parallel}$ normalized to its zero-crystal-field value as a function of $\Delta/T_K^{(8)}$ is shown for case (a) in Fig. 3(a) and for case (b) in Fig. 4. Note that the susceptibility in each case has a universal dependence on $\Delta/T_K^{(8)}$. The Wilson ratio in the large-crystal-field-splitting limit becomes $\chi/\gamma=3/2\pi^2$ in case (a) and $\chi/\gamma=49(3/2\pi^2)$ in case (b). This value is twice as large as for free electrons and is the expected Wilson ratio for a spin-$\frac{1}{2}$ impurity, $(\chi/\mu^2)/(3\gamma/\pi^2)=2$.

It is somewhat more tedious to obtain $\chi_{\perp}$, since for our choice of crystal-field levels the Zeeman and crystal-field Hamiltonians do not commute with each other. This gives rise to van Vleck contributions. For both of our examples the magnetic field has only nonvanishing matrix elements between states whose j_z quantum numbers m differ by ±1. The ionic energy matrix (crystal field and Zeeman) is diagonalized and the energy eigenvalues are expanded in powers of the magnetic field. Only terms up to order H^2 are needed to get the transverse susceptibility. For case (a) we obtain

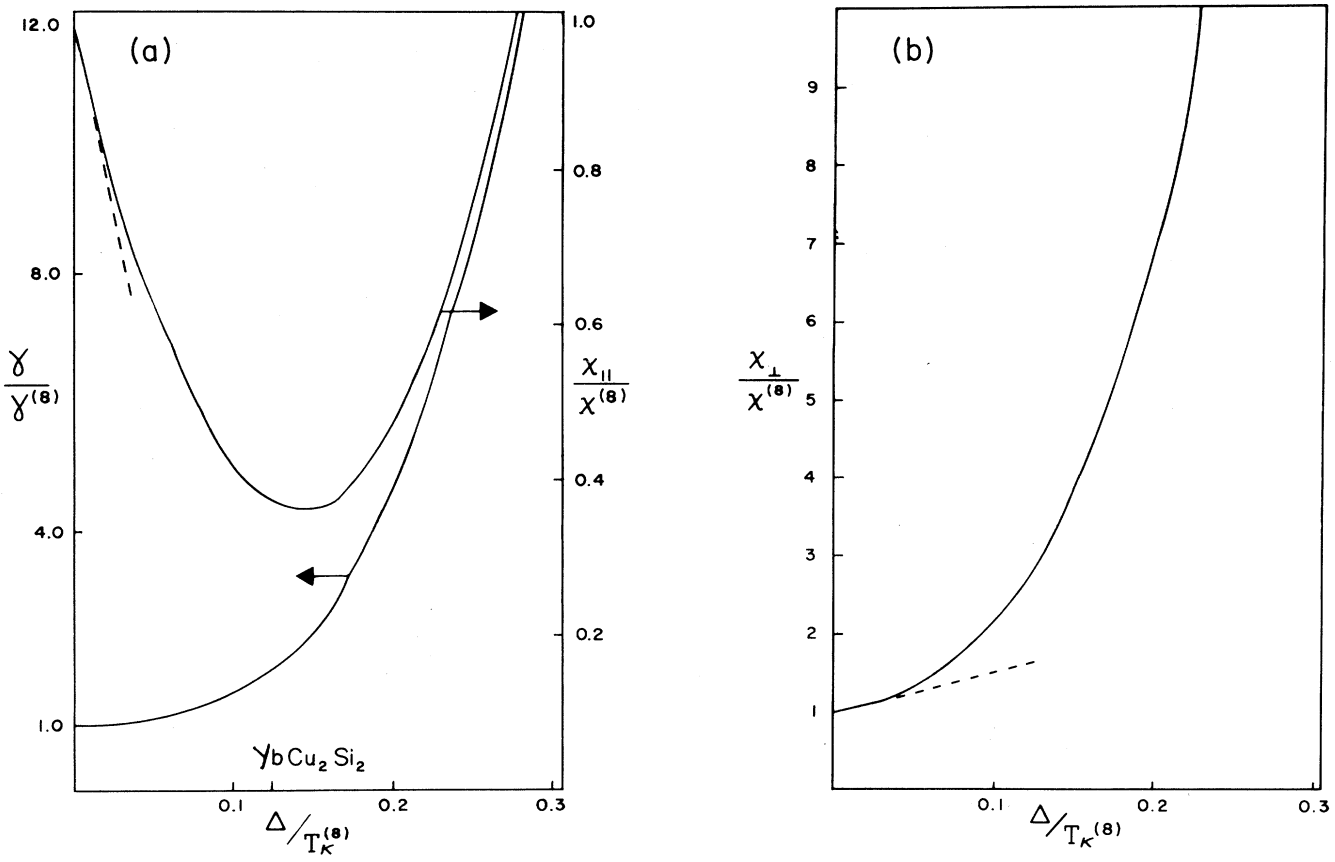

FIG. 3. Linear temperature coefficient of the specific heat γ over its value in the absence of crystal-field splitting and magnetic susceptibility for the field (a) parallel to the crystal field axis, $\chi_{\parallel}$, and (b) perpendicular to it, $\chi_{\perp}$, as a function of $\Delta/T_K^{(8)}$. The susceptibilities are normalized to its value in the absence of crystal fields, $\chi^{(8)}$, and correspond to the crystal-field levels arranged as $\pm\frac{1}{2}$, $\pm\frac{3}{2}$, $\pm\frac{5}{2}$, and $\pm\frac{7}{2}$, in increasing order of their energies. A dash indicates our estimate of the crystal-field parameter for $YbCu_2Si_2$.

$$S_z=2\int_{-\infty}^{\infty}d\xi\,\sigma^{(1)}(\xi)+\left[15\int_{-\infty}^{\infty}d\xi\,\sigma^{(2)}(\xi)+6\sqrt{2}\int_{-\infty}^{\infty}d\xi\,\sigma^{(4)}(\xi)+7\int_{-\infty}^{\infty}d\xi\,\sigma^{(6)}(\xi)\right]\frac{H}{4\Delta} \tag{4.18a}$$

and for case (b)

$$S_z=2\int_{-\infty}^{\infty}d\xi\,\sigma^{(7)}(\xi)+\left[7\int_{-\infty}^{\infty}d\xi\,\sigma^{(2)}(\xi)+6\sqrt{2}\int_{-\infty}^{\infty}d\xi\,\sigma^{(4)}(\xi)+15\int_{-\infty}^{\infty}d\xi\,\sigma^{(6)}(\xi)\right]\frac{H}{4\Delta}\ . \tag{4.18b}$$

Following the procedure outlined before we get

$$\chi_\perp=2^{3/2}[e^{\pi(B+1/J)}+\hat{\sigma}^{(2)}_{h\,\mathrm{imp}}(i\pi)]/\varepsilon_F\hat{\rho}_{1h\,\mathrm{host}}(i\pi)+[15\hat{\sigma}^{(2)}_{\mathrm{imp}}(0)+6\sqrt{2}\hat{\sigma}^{(4)}_{\mathrm{imp}}(0)+7\hat{\sigma}^{(6)}_{\mathrm{imp}}(0)]/4\Delta \tag{4.19a}$$

for case (a), and similarly, for case (b)

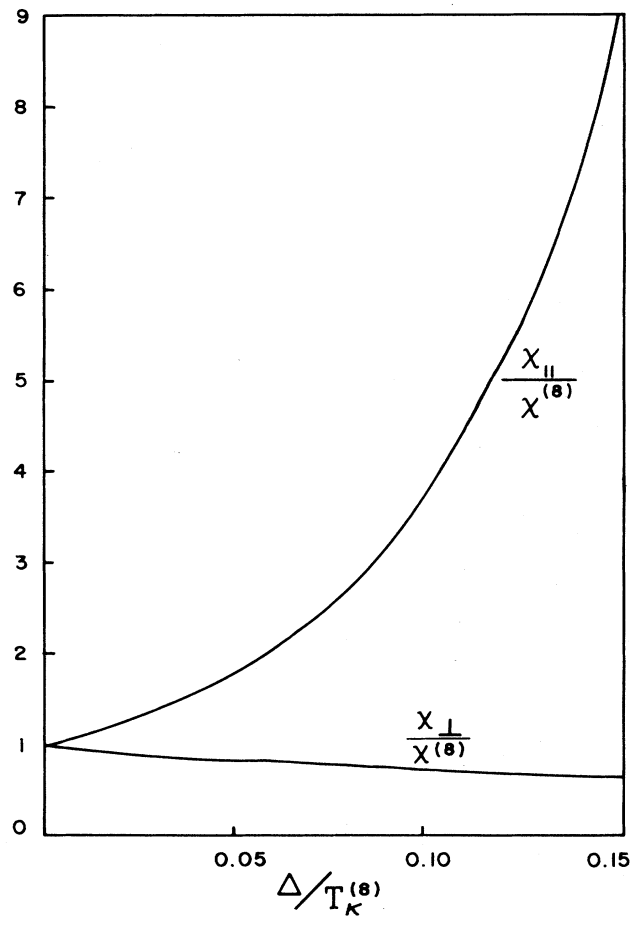

FIG. 4. Anistropic magnetic susceptibility normalized to its zero-crystal-field value as a function of $\Delta/T_K^{(8)}$ for the Kramers doublets having the following magnetic quantum numbers: $\pm\frac{7}{2}$, $\pm\frac{5}{2}$, $\pm\frac{3}{2}$, and $\pm\frac{1}{2}$, in increasing order of their energies.

$$\chi_\perp=2^{3/2}\hat{\sigma}^{(6)}_{h\,\mathrm{imp}}(i\pi)/\varepsilon_F\hat{\rho}_{1h\,\mathrm{host}}(i\pi)+[7\hat{\sigma}^{(2)}_{\mathrm{imp}}(0)+6\sqrt{2}\hat{\sigma}^{(4)}_{\mathrm{imp}}(0)+15\sigma^{(6)}_{\mathrm{imp}}(0)]/4\Delta\ . \tag{4.19b}$$

The first term in (4.19a) and (4.19b) is due to the Zeeman splitting of the Kramers doublet. Note that this Kramers doublet (within our choice of crystal-field levels) is the only one split by a transverse magnetic field. The remaining terms with Δ in the denominator are van Vleck contributions. For small Δ expressions (4.19) reduces to the isotropic susceptibility of the Coqblin-Schrieffer model, $\chi^{(8)}=21/4T_K^{(8)}$. Again, (4.19a) and (4.19b) are universal functions of $\Delta/T_K^{(8)}$ which are displayed in Figs. 3(b) and 4, respectively. Their dependence on Δ is very different, which is due to the exponential term present in case (a) but absent in case (b). The origin of this term is the same as for the analogous terms in γ and $\chi_\parallel$, namely the Kondo effect of the lowest-lying Kramers doublet. The term is inversely proportional to $T_K^{(2)}$, Eq. (4.15). This term is absent in case (b), since a transverse magnetic field cannot split the lowest-lying Kramers doublet $m=\pm\frac{7}{2}$, because the matrix element connecting the two states vanishes.

Contrary to the common belief, for sufficiently large splitting, the Kondo effect only appears for the lowest-lying Kramers doublet, but not for the excited doublets. In addition, the susceptibility only shows a Kondo term if the lowest-lying Kramers doublet is actually split by the magnetic field (see also Ref. 10).

V. DISCUSSION AND COMPARISON WITH EXPERIMENTS

We considered an Yb^{3+} ion in an axial crystal field, such that the excited Kramers doublets have energies Δ, $(1+\sqrt{2})\Delta$, and $(2+\sqrt{2})\Delta$. Under these conditions the exact solution of the Coqblin-Schrieffer model can be obtained analytically. The results display a universal dependence on $\Delta/T_K^{(8)}$, where $T_K^{(8)}$ is the Kondo temperature of the Yb^{3+} octuplet. The population of the Kramers doublets is shown in Fig. 1 as a function of the crystal-field splitting and in Fig. 2 we present the crystal-field response function defined by Eq. (3.10). Note that this response is linear up to about $\Delta/T_K^{(8)}=0.15$. The ground state is a singlet for all values of Δ. As a consequence the impurity specific heat at low temperatures is linear in T. The specific-heat coefficient γ is displayed in Fig. 3(a) as a function of $\Delta/T_K^{(8)}$. Note that for small splitting $\gamma(\Delta)$ increases as Δ^2 while for large Δ it increases as Δ^3. This increase of is due to the gradual reduction of the degeneracy of the f level. The occupation numbers, the correlation function $q(\Delta)$, and $\gamma(\Delta)$ are all independent of the magnetic quantum numbers associated with the Kramers doublets. This is not the case for the magnetic response.

As a consequence of the axial crystal field, the magnetic susceptibility is anisotropic, i.e., $\chi_\parallel\neq\chi_\perp$. In addition, it depends on the magnetic quantum numbers of each Kramers doublet. We considered two cases: in Fig. 3 we associated $\pm\frac{1}{2}$, $\pm\frac{3}{2}$, $\pm\frac{5}{2}$, and $\pm\frac{7}{2}$ with the doublets in decreasing order of population and the inverse order in Fig.

4. $\chi_{\parallel}$ always increases as a function of Δ due to the Kondo effect in the ground multiplet with reduced degeneracy (T_K shows the crossover from $T_K^{(8)}$ to $T_K^{(2)}$), while $\chi_{\perp}$ only shows a Kondo term if there is a matrix element with the Zeeman Hamiltonian that lifts the degeneracy of the lowest-lying Kramers doublet, present for the case displayed in Fig. 3, but absent in the case shown in Fig. 4. This property of axial crystal fields has been found previously for Ce ions.[10] Note that only the lowest-lying Kramers doublet may give rise to a Kondo exponential term, not the excited Kramers doublets.

Finally, we would like to use our results for a comparison with experiments. We consider systems with relatively small crystal-field splittings compared to the Kondo temperature of the octuplet. Two such systems are $YbCu_2Si_2$ and YbCuAl, which crystallize in tetragonal and hexagonal structures, respectively. The quanitity of primary interest is the quadrupolar moment of the Yb^{3+} $4f$ shell, $Q(T)$. This quadrupolar moment is induced by the lattice symmetry via the crystalline fields and can be measured by means of the Mössbauer effect.

Assume first that the crystal-field strength Δ for the system under consideration is such that it belongs to the linear regime of $q(\Delta)$ (see Fig. 2), i.e., $\Delta/T_K^{(8)} \leq 0.15$. Under these circumstances linear response with respect to the crystal fields is valid. The range of validity of linear response is expected to grow with temperature, as a consequence of the smearing of the Kondo resonance. Hence, in linear response we have for all temperatures that

$$Q(T)/Q(0)=\chi(T)/\chi(0) , \tag{5.1}$$

where $\chi(T)$ is the magnetic susceptibility of the degenerate octuplet. This result holds for *arbitrary* crystal-field splitting, as long as it is small compared to $T_K^{(8)}$, even in the mixed-valent regime. $\chi(T)$ has been obtained previously by numerically solving the thermodynamic Bethe-*Ansatz* equations[16] for the degenerate Anderson model with excluded double occupancy of the f level. Both the experimental data[17] for $Q(T)$ and the $\chi(T)$ curves for various valence admixtures[16] show a maximum as a function of T. Defining the Kondo temperature via $\chi(0)=j(j+1)/3T_K^{(8)}$ also if there is some valence admixture, we find that the temperature T_m at which $\chi(T)$ is maximum is proportional to $T_K^{(8)}$ over a large regime of parameters ε (f-level energy with respect to the Fermi energy) and $\Gamma=\pi\rho V^2$, Γ being the hybridization width. It is then natural to adjust $T_K^{(8)}$ so that the position of the maxima of experiment and theory coincide. For $YbCu_2Si_2$ this yields $T_K^{(8)}=357$ K (see Fig. 5). The value of the susceptibility at the maximum, i.e., $\chi(T_m)/\chi(0)$, is not universal but depends on the valence admixture.

Further input is necessary to determine other energy parameters for $YbCu_2Si_2$. The electric field gradient as measured by the Mössbauer effect is a superposition of at least two contributions; one due to the quadrupolar moment of the lattice which is expected to be almost temperature independent, the other arising from the quadrupolar crystal-field splitting of the Yb $4f$ shell. This latter contribution is temperature dependent. These two contributions to $Q(0)$ cannot be separated experimentally,

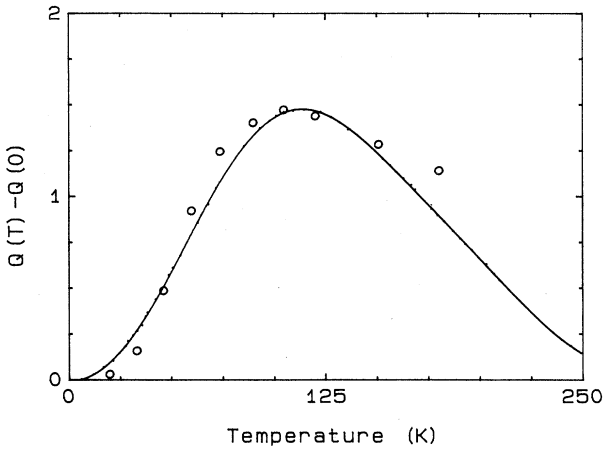

FIG. 5. Temperature-dependent quadrupole moment $Q(T)$ of the Yb $4f$ shell in $YbCu_2Si_2$. The experimental points are taken from Ref. 17 and the curve is our fit with the parameters given in the text.

but $Q(T)$ in (5.1) only refers to the f-shell part.

The valence admixture of the $4f^{14}$ configuration has been determined by L_{III} x-ray-absorption measurements.[18] At low T the average $4f$-hole expectation[18] is $n_f=0.82$. We use this result to determine the second energy parameter of the Anderson model, i.e., $\Gamma=714$ K and $(\varepsilon-A)/\Gamma=-4.05$. Note that $n_f(0)$ is only weakly dependent on the crystal-field splitting,[7] in particular if this splitting is small, as assumed here (there is no linear change of n_f with the crystal field, since the trace of Stevens operators vanishes). The temperature dependence of n_f for the above parameters of Anderson's model is shown in Fig. 6.

The ratio of $\chi(T_{\max})/\chi(0)$ for the above parameters[16] is 1.37, so that the $4f$ contribution to the quadrupolar moment can be determined from $Q(T_{\max})-Q(0)$, $Q(0)=4.04$. The quadrupolar splitting caused by the $4f$ shell is then $\Delta E_Q(T)=KQ(T)$, where $K=0.647$ mm/sec for ^{174}Yb. At $T=0$ this amounts to $\Delta E_Q(0)=2.61$

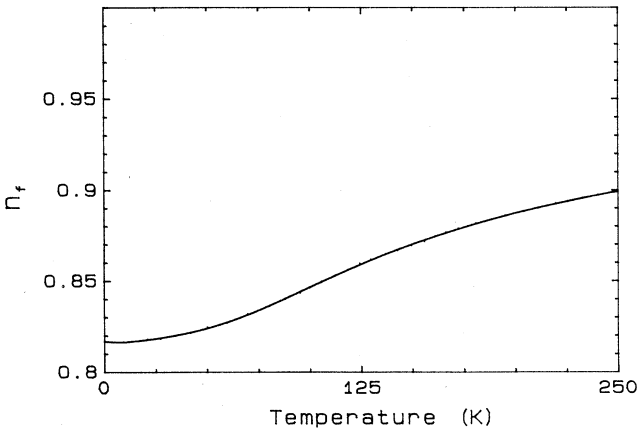

FIG. 6. Temperature dependence of the f-hole occupation of Yb in $YbCu_2Si_2$. The parameters are given in the text.

mm/sec arising from the $4f$ shell. The total splitting measured at 4 K is $\Delta E(4\text{ K})=0.946$ mm/sec,[17] such that the lattice contribution to the quadrupolar splitting is then $\Delta E_{Q\,\text{latt}}=-1.67$ mm/sec.

The measured value[19,20] of the specific-heat coefficient γ is 135 mJ/mole K^2. This value, normalized for one Yb atom, corresponds to $\gamma=0.0162$/Yb-atom K. On the other hand, using (4.9) and $T_K^{(8)}=357$ K we obtain $\gamma^{(8)}=0.000\,806$/K. Hence crystal fields enhance γ by about a factor of 2. This enhancement can be used to get an estimate of Δ. From Fig. 3(a) we have that $\Delta/T_K^{(8)}$ is approximately 0.125, i.e., $\Delta=44.6$ K. Note that this value of $\Delta/T_K^{(8)}$ is still within the linear regime of the response function (see Fig. 2). This proves our assumption that linear response with respect to the crystal field is valid for the system $YbCu_2Si_2$.

As already discussed in Sec. IV, the anisotropic magnetic susceptibility depends strongly on the wave functions associated with the Kramers doublets. For example, in tetragonal symmetry there are five Stevens operators contributing to the crystal-field splitting, i.e., there are five independent fine-structure coefficients to determine three energy differences. The character of the wave functions can then not be determined from the energy spectrum. We limit ourselves to discussing the two cases discussed Sec. IV. From Fig. 3 (the ground doublet corresponds to $m=\pm\frac{1}{2}$) we obtain, for $\Delta/T_K^{(8)}=0.125$, that $\chi_\parallel/\chi^{(8)}=0.37$ and $\chi_\perp/\chi^{(8)}=2.86$. Since $\chi^{(8)}=g^2 21/4T_K^{(8)}=0.0192$ K^{-1}, where $g=\frac{8}{7}$ is the Yb^{3+} g factor, we have $\chi_\parallel=0.0071$ K^{-1} (0.002 66 emu/mol) and $\chi_\perp=0.055$ K^{-1} (0.0206 emu/mol). In this case $\chi_\perp/\chi_\parallel\gg1$ contrary to the experimental observation.[19,21] On the other hand, if the ground doublet corresponds to $m=\pm\frac{7}{2}$ we obtain from Fig. 4 that $\chi_\perp/\chi^{(8)}=0.67$ and $\chi_\parallel/\chi^{(8)}=5.57$, yielding $\chi_\perp=0.0128$ K^{-1} (0.0048 emu/mol) and $\chi_\parallel=0.107$ K^{-1} (0.040 emu/mol). Here $\chi_\perp/\chi_\parallel=0.12$, while the best experimental estimate[21] is $\chi_\perp/\chi_\parallel=0.3$ with $\chi_\parallel\sim0.028$ emu/mol. Our estimate of $\chi_\parallel$ and $\chi_\perp$ gives the correct order of magnitude and should be considered as an upper bound. The result is very sensitive to the magnetic character of the ground doublet: a crystal-field admixture of the $\pm\frac{7}{2}$ states with the $+\frac{1}{2}$ necessarily reduces $\chi_\parallel$ and increases $\chi_\perp$.

In summary we have shown that most of the available data for $YbCu_2Si_2$ can be explained with a relatively small crystal-field splitting. The temperature dependence of $Q(T)$ is due to the gradual population and smearing of the Kondo resonance. Coherence effects within the Kondo lattice only seem to play a minor role. A similar explanation has been previously proposed by Zevin *et al.*[17] Our energy parameters are close to the values employed by them, e.g., their energy difference between the two lowest-lying Kramers doublet is 39 K as compared to $\Delta=45$ K and their value of Γ is 550 K, while we obtain $\Gamma=714$ K. Now variations of Γ can be absorbed into a change of ε, keeping $T_K^{(8)}$ invariant. Their dressed (by the crystal-field splitting) Kondo temperature is 200 K, while our bare Kondo temperature is $T_K^{(8)}=357$ K. Our dressed T_K can be estimated from the γ coefficient to be of the order of 180 K. Our quadrupolar moment due to the $4f$ shell, $Q(0)$, is roughly 10% larger than in Ref. 17.

An analogous analysis can be performed for the quadrupolar splitting[22] in YbCuAl. For this compound a very good agreement of the impurity theory with the data for the field dependence of the low-temperature magnetization,[11] the temperature dependence of the specific heat and the susceptibility,[16] as well as for the valence[16], has been obtained. The main parameter is the bare Kondo temperature $T_K^{(8)}=100$ K (note that the T_K of 66 K of Ref. 11 when rescaled into the definition of $T_K^{(8)}$ used here corresponds to 98 K). The fits in Ref. 16 were obtained with $\Gamma=527$ K and $(\varepsilon-A)/\Gamma=-10.2$. Again, as a consequence of the Kondo resonance $Q(T)$ increases[22] as a function of T. The amplitude, i.e., $Q(0)$, is smaller in this case since crystal fields are less important for this compound than for $YbCu_2Si_2$. With the above parameters the theoretical curve has its maximum at about 40 K. The experimental data do not follow this trend and stay above the theoretical curve for the higher temperatures, similar to those for $YbCu_2Si_2$. Note that the Mössbauer measurements for YbCuAl were performed on a different isotope, namely ^{170}Yb. We converted the energies in Fig. 1 of Ref. 22 into effective quadrupolar moments, the conversion factor being $K=0.28$ mm/sec. The data for $YbCu_2Si_2$ of Refs. 17 and 22 then agree within 10%. The data for YbCuAl of Ref. 22 are shown in Fig. 7, together with the theoretical curve obtained via (5.1) using $\chi(T)$ from Ref. 16. Our estimation of $Q(0)$ is 1.75 so that the quadrupolar splitting at $T=0$ arising from the Yb^{3+} f shell is $\Delta E_Q=0.50$ mm/sec. Since the total quadrupolar splitting is -0.75 mm/sec we have that the lattice contribution is approximately -1.25 mm/sec.

It is worth pointing out that the discrepancy between theory and experiment for $Q(T)$ at higher temperatures may be due to experimental difficulties. The recoil-free fraction of the γ-emission f is proportional to

$$f\sim\exp[-E_\gamma^2\langle x^2\rangle/(hc)^2]\ ,$$

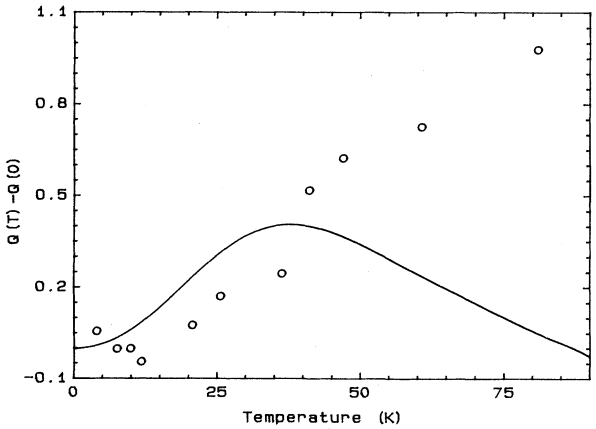

FIG. 7. Temperature-dependent quadrupole moment $Q(T)$ of the Yb $4f$ shell in YbCuAl. The experimental data are from Ref. 22 and the curve is the fit to the magnetic susceptibility for the same compound taken from Ref. 16. The parameters are given in the text.

where E_γ is the energy of the photon and $\langle x^2 \rangle$ is the mean square displacement of the atoms. Both Yb isotopes, ^{170}Yb and ^{174}Yb, have large E_γ energies of 78 and 84 keV, respectively, so that f is small. The recoilless fraction f decreases further with temperature, since $\langle x^2 \rangle$ grows, so that measurements become difficult.

ACKNOWLEDGMENTS

We would like to thank the U.S. Department of Energy for their support under Grant No. DE-FG02-87ER45333.

*Present address: Department of Physics, University of Michigan, Ann Arbor, MI 48109.

[1]A. M. Tsvelick and P. B. Wiegmann, J. Phys. C **15**, 1707 (1982).

[2]J. W. Rasul, in *Valence Instabilities,* edited by P. Wachter and H. Boppart (North-Holland, Amsterdam, 1982), p. 49.

[3]N. Andrei, K. Furuya, and J. H. Lowenstein, Rev. Mod. Phys. **55**, 331 (1983).

[4]P. Schlottmann, Z. Phys. B **51**, 49 (1983).

[5]P. Schlottmann, Z. Phys. B **55**, 293 (1984).

[6]N. Kawakami and A. Okiji, in *Theory of Heavy Fermions and Valence Fluctuations,* edited by T. Kasuya and T. Saso (Springer-Verlag, Heidelberg, 1985), p. 57.

[7]P. Schlottmann, Phys. Rev. B **30**, 1454 (1984).

[8]H.-U. Desgranges and J. W. Rasul, Phys. Rev. B **32**, 6100 (1985).

[9]H.-U. Desgranges and J. W. Rasul, Phys. Rev. B **36**, 328 (1987).

[10]P. Schlottmann, J. Magn. Magn. Mater. **52**, 211 (1985).

[11]A. C. Hewson and J. W. Rasul, J. Phys. C **16**, 6799 (1983).

[12]K. R. Lea, M. J. M. Leask, and W. P. Wolf, J. Phys. Chem. Solids **23**, 1381 (1962).

[13]P. M. Morse and H. Feshbach, *Methods of Theoretical Physics* (McGraw-Hill, New York, 1953).

[14]N. Kawakami and A. Okiji, J. Phys. Soc. Jpn. **54**, 685 (1985).

[15]K. Yamada, K. Hanzawa, and K. Yosida, Prog. Theor. Phys. **71**, 450 (1984).

[16]P. Schlottmann, Z. Phys. B **57**, 23 (1984).

[17]V. Zevin, G. Zwicknagl, and P. Fulde, Phys. Rev. Lett. **60**, 2331 (1988).

[18]G. Neumann, J. Langen, H. Zabel, D. Plumacher, Z. Kletowski, W. Schlabitz, and D. Wohlleben, Z. Phys. B **59**, 133 (1985).

[19]B. C. Sales and R. Viswanathan, J. Low Temp. Phys. **23**, 449 (1976).

[20]R. Kuhlmann, H.-J. Schwann, R. Pott, W. Boksch, and D. Wohlleben, in *Valence Instabilities,* edited by P. Wachter and H. Boppart (North-Holland, Amsterdam, 1982), p. 455.

[21]T. Shimizu, J. Yasuoka, Z. Fisk, and J. L. Smith, J. Phys. Soc. Jpn. **56**, 4113 (1987).

[22]P. Bonville and J. A. Hodges, J. Magn. Magn. Mater. **47+48**, 152 (1985).